Vol. 20, No. 1 (2021) 453-466
Revista Mexicana de Ingeniería Química

Molecular docking of oxidases from *Pleurotus ostreatus* and the activity of those produced by ARS 3526 strain grown in both, submerged and solid-state fermentations

Acoplamiento molecular de oxidasas de *Pleurotus ostreatus* y la actividad de estas producidas por la cepa ARS 3526 crecida tanto en fermentación sumergida como fermentación en estado sólido

L.D. Herrera-Zúñiga[3], M. González-Palma[2], G. Díaz-Godínez[1], D. Martínez-Carrera[4], C. Sánchez[3], R. Díaz[1]*

[1]*Laboratory of Biotechnology, Research Center of Biological Sciences, Autonomous University of Tlaxcala, Mexico*
[2]*Master in Biological Science, Autonomous University of Tlaxcala*
[3]*Division of Environmental Engineering Technology of Higher Studies of East Mexico State, Mexico state, Mexico.*
[4]*Biotechnology of Edible, Functional and Medicinal Mushrooms, College of Postgraduates, Puebla Campus, Puebla, México*

Received: September 30, 2020; Accepted: December 8, 2020

Abstract

Pleurotus ostreatus is a basidiomycete fungus capable of producing oxidases involved in the degradation of lignin, such as laccase (Lac), manganese peroxidase (MnP), versatile peroxidase (VP), veratryl alcohol oxidase (VAO) and dye-decolorizing peroxidase (DyP). In this research, the molecular docking showed that the interaction between Mn-ion, ABTS or DMP ligand with the respective oxidases studied were strongly supported by exposed GLU and ASP charged residues H-bonded or hydrophobic-bonded, in most of the complexes, mainly GLU and ASP played a very important role in the union, especially in the presence of the Mn-ion. On the other hand, the growth and activity of such enzymes of *Pleurotus ostreatus* ARS 3526 grown in both, submerged fermentation (SmF) and solid-state fermentation (SSF) were evaluated. The specific growth rate in SSF was 2.5 times higher than in SmF. The values of activity of Lac, VP and DyP were higher in the SSF, of the VAO activity was similar in both fermentation systems and SmF had the higher MnP activity value in comparison with SSF. This study provides evidence of the enzymatic potential of this fungus and shows the similarities in charged amino acids when used in their catalytic interactions, and the intimate relationship between the enzyme and its substrate.

Keywords: Molecular docking, oxidases, enzymatic activity, *Pleurotus ostreatus*.

Resumen

Pleurotus ostreatus es un hongo basidiomicete capaz de producir oxidasas involucradas en la degradación de la lignina, tales como Lacasa (Lac), Manganeso Peroxidasa (MnP), Versátil Peroxidasa (VP), Veratríl Alcohol Oxidasa (VAO) y Decolorante Peroxidasa (DyP). En esta investigación, el acoplamiento molecular mostró que la interacción entre el ión Mn, o ligandos de ABTS o DMP con las respectivas oxidasas estudiadas, está fuertemente apoyada por residuos expuestos de GLU y ASP cargados con enlaces de H o con enlaces hidrófobos, en la mayoría de los complejos, principalmente GLU y ASP jugaron un papel muy importante en la unión, especialmente en presencia del ion Mn. Por otro lado, se evaluó el crecimiento y la actividad de dichas enzimas de *Pleurotus ostreatus* ARS 3526 cultivado en fermentación sumergida (SmF) así como en fermentación en estado sólido (SSF). La tasa de crecimiento específico en SSF fue 2,5 veces mayor que en SmF. Los valores de actividad de Lac, VP y DyP fueron mayores en el SSF, la actividad de VAO fue similar en ambos sistemas de fermentación y SmF tuvo el valor de actividad de MnP más alto en comparación con SSF. Este estudio proporciona evidencia del potencial enzimático de este hongo y muestra las similitudes en los aminoácidos cargados cuando se usan en sus interacciones catalíticas, y la íntima relación entre la enzima y su sustrato.

Palabras clave: Acoplamiento molecular, oxidasas, actividad enzimática, *Pleurotus ostreatus*.

1 Introduction

New computational methodologies allow analysis of the interactions between a target protein and a ligand, which through different algorithms can simulate biological systems to create new paradigms in computing, such as neural networks or evolutionary computing (Heberle and de Azevedo, 2011).

* *Corresponding author. E-mail*: 2803pleurotusos@gmail.com
https://doi.org/10.24275/rmiq/Bio2076
ISSN:1665-2738, *issn-e*: 2395-8472

Molecular docking is a tool used in structural biology and computer-aided drug design. The goal of ligand-protein coupling is to predict the binding mode of a ligand with a protein of known three-dimensional structure; molecular docking can be used to perform virtual screening on large compound libraries, classify results, and propose structural hypotheses between ligands (Morris and Lim-Wilby, 2008). Molecular docking methodology explores the behavior of small molecules at the binding site of a target protein, largely accomplished because more protein structures are experimentally determined by X-ray crystallography or nuclear magnetic resonance (NMR) spectroscopy. Docking of homology-modeled target molecules is also possible for proteins whose structures are not known as well as the driving forces of these specific interactions in biological systems that will allow complementarity between the shape and electrostatics of the surfaces of the binding site and the ligand (Pagadala *et al*., 2017). The molecular docking between the active site of the enzymes and specific substrates allows knowing the detail of the ligands, in order to propose evolutionary changes or modifications by means of protein engineering to make them more resistant to changes in pH or temperature, reducing the thermodynamic energy of protein structures (Díaz *et al*., 2018a; Díaz *et al*., 2018b).

It is important to mention that in the last century, a wide variety of chemical products with a high pollutant and recalcitrant potential have been developed, such as pesticides, dyes and industrial process wastes, such as effluents from the paper-producing industry and the textile industry that end up in rivers and lakes by intentionally. The use of fungal enzymes in effluent bioremediation is an alternative to transform polluting chemical compounds into simple substances, reducing their negative effect on the ecosystems that have contact with said effluents (Knapp *et al*., 1995; Hernández-Ruiz *et al*., 2017). In that sense, the ligninolytic system of white-rot fungi such as *Pleurotus ostreatus, Phanerochaete chrysosporium, Pycnoporus cinnabarinus* and *Trametes versicolor* has been extensively studied in the effluent recovery from the paper, textile and chemical industries (Rothschild *et al*., 1999; Ullah *et al*., 2000; Herrera-Mora *et al*., 2004; Ruiz-Dueñas *et al*., 2013; Martínez-Restrepo, 2014; Villegas *et al*., 2016). These ligninolytic enzymes can act separately or together (Dávila-Vázquez *et al*., 2005). Fungi of the genus Pleurotus produce different ligninolytic enzymes, which due to their catalytic activity are classified as oxidases, therefore, these organisms have a potential use in bioremediation processes (Montoya *et al*., 2014).

The main activity of oxidase enzymes from *Pleurotus ostreatus* is represented by laccase (Lac), manganese peroxidase (MnP), versatile peroxidase (VP), veratryl alcohol oxidase (VAO) and dye-decolorizing peroxidase (DyP), that have been produced in submerged fermentation (SmF) and solid-state fermentation (SSF) (Cuamátzi-Flores *et al*., 2015, Álvarez *et al*., 2016; Medina *et al*., 2017; Olvera-García *et al*., 2017). Many studies have suggested that the production of these enzymes as well as the rate grown of fungi are influenced by multiple environmental factors like pH, temperature, composition and inductors of the culture medium (Téllez-Téllez *et al*., 2008; Díaz *et al*., 2013; Montalvo *et al*., 2020; Valenzuela-Cobos *et al*., 2020). Based on the above, it is very important to try to know the interactions of enzymes with their substrates through molecular docking, without forgetting that computational models must complement what is observed *in vivo*. For this reason, in this research the molecular coupling of oxidases from *Pleurotus ostreatus* was carried out for the first time and the production of these enzymes by the strain ARS 3526 cultivated in both SmF and SSF was characterized, which will contribute to the generation of knowledge about the capacity of this organism to produce these oxidases and the molecular coupling of each protein with its ligand.

2 Materials and methods

2.1 Molecular docking

Molecular docking was performed using X-ray structures from *Pleurotus ostreatus* of MnP (PDB-ID:4BM1), VP (PDB-ID: 4BLK) (Fernández-Fuello *et al*., 2014), DyP (PDB-ID:6FSL) (Romero *et al*., 2019) and Lac (Lacc 6 protein structure was taken of Díaz *et al*., 2018a). The 2,2'-azino-bis (3-ethylbenzothiazoline-6-sulfonic acid) (ABTS) and 2,6- dimethoxyphenol (DMP) structures were taken from PubChem database. The docking studies of enzymes were performed using AutoDock 4.2.6 software (v 4.2.6 supported by The Scripps Research Institute U. S. A.) (Morris *et al*., 2009). Many enzymes have metal ions in their active sites that play key roles in substrate binding and catalysis. Particularly,

in MnP and VP, manganese sulfate interactions were docked as Mn^{2+} ions, and were carried out according to the protocol established by Chen *et al*., 2007, who carried out the docking of adenylyl cyclase toxins of mammal, with Mg^{2+} and Zn^{2+} ions in their active sites. The initial configuration was built considering the farthest distances between the ligands of each protein structure, the number of torsional degrees of freedom in the ligands were six.

The Lamarckian genetic algorithm was used to run Autodock with 250 random orientations for each substrate, simulations were carried out considering 2.5 $\times 10^6$ evaluations with a maximum of 2.5 $\times 10^4$ generations. Each simulation was performed 1000 times. Each ligand was prepared automatically in AutoDock with flexible torsions, and space docking by ligand movements was fixed, considering the enzyme centered inside a grid box comprised of 126 × 126 × 126 grid points with a space between each grid point of 0.385 Å. The search for binding modes was done using AutoDock through the flexible residues that were present for each enzyme. Flexible amino acids were chosen in consideration of the Computed Atlas of Surface Topography of Proteins v 3.0 (CASTp) (Tian *et al*., 2018), CAVER Analyst 2.0 from National Center for Biotechnology Information, U. S. National Library of Medicine (Jurcik *et al*., 2018) and Active site in UniProt analysis (UniProt Consortium, 2019). Parameters for heme group and copper were adapted and included in AD4_parameters file, according to the AutoDock user guide. Chimera software (UCSF Chimera 2004) supported by the National Institutes of Health (Pettersen *et al*., 2004) was used to rebuild DyP wildtype and to visualize the docking results. Ligplot+ software supported by European Bioinformatics Institute, Cambridgeshire, U. K. (EMBL-EBI) was used to build the 2D diagram interactions (Wallace *et al*., 1995). The computational analysis (modeling and docking) was not performed on VAO because no sequences deposited in the protein databases were found.

2.2 *Organism*

A strain of *Pleurotus ostreatus* from Agricultural Research Service (ARS 3526) (U.S.A.) was used. The strain was grown on potato dextrose agar (PDA) (SIGMA Aldrich^R) at 25 ºC for 7 days and kept at 4 ºC until its use.

2.3 *Conditions of the culture of Pleurotus ostreatus and biomass evaluation*

Three mycelial plugs (4 mm diameter) taken from the periphery of colonies of *Pleurotus ostreatus* grown as indicated previously were used as inoculum in each experimental unit in both fermentation systems. The culture medium composition used in all cases was reported by Téllez-Téllez *et al*., (2008). Erlenmeyer flasks of 125 mL containing 50 mL of culture medium were used for SmF, the incubation was carried out at 25ºC with orbital shaking (120 rpm). The SSF was carried out using Erlenmeyer flasks of 250 mL containing 0.5 g of polyurethane foam of low density (PUF; 17 kg/m^3) cubes (0.5 cm per side) as an inert support impregnated with 15 mL of culture medium (Díaz-Godínez *et al*., 2001). Both bioprocesses were sampled by triplicate each 24 h during 528 h and 384 h for the SmF and SSF, respectively. The culture medium obtained from each sample was considered the enzymatic extract (EE), for the SmF it was obtained by filtration (Wathman No. 4) retaining the biomass, in the case of the SSF, the PUF was pressed into a 50 mL syringe, the biomass was fixed in the PUF, in both cases the biomass (X) was determined as the difference of dry weight (gL^{-1}) (Díaz-Godínez *et al*., 2001).

The assay of biomass $X = X(t)$ was done using the Velhurst-Pearl logistic equation,

$$\frac{dX}{dt} = \mu\left[1 - \frac{X}{X_{max}}\right]X \tag{1}$$

where, μ is the maximal specific growth rate, and X_{max} is the maximal (or equilibrium) biomass level achieved when $dX/dt = 0$ for $X > 0$. The solution of above equation is the following,

$$X = \frac{X_{max}}{1 + Ce^{-\mu t}} \tag{2}$$

where, $C = (X_{max} - X_0)/X_0$; being $X = X_0$; the initial biomass value.

Estimation of kinetic parameters in the previous equation was done using a non-linear least square-fitting program called "Solver", present in Excel electronic sheet (Microsoft) (Díaz-Godínez *et al*., 2001).

2.4 *Enzyme assay*

For all enzymes, activity was reported in international units (U, amount of enzyme that is required to oxide one μmol of substrate per minute in the reaction

mixture), but Lac activity was also informed in arbitrary units (AU, amount of enzyme that is required to increase the absorbance in one unit in the reaction mixture). Lac activity was measured in the reaction mixture that contained 950 μL substrate (2 mM DMP in 0.1 M phosphate buffer, pH 6.5) and 50 μL of EE, after one min of incubation the absorbance was read at 468 nm (ε= 35645 cm^{-1} M^{-1}) (Grandes-Blanco *et al*., 2013). The MnP activity was determined in the assay mixture, containing 850 μL of substrate (0.5 mM manganous sulphate in 50 mM sodium malonate buffer, pH 4.5), 100 μL of EE and 50 μL of 0.05 mM H_2O_2, incubated at 30ºC for one minute, after that the absorbance at 270 nm (ε=11590 cm^{-1} M^{-1}) was read (Giardina *et al*., 2000). The VP activity was obtained through an assay mixture, containing 850 μL of substrate (20 mM manganese sulphate in 0.1 M sodium tartrate buffer, pH 5.0), 50 μL of 0.1 mM H_2O_2 and 100 μL of EE. VP activity was followed by an absorbance increase at 238 nm (ε=6500 cm^{-1} M^{-1}) (Rodríguez *et al*., 2004; Pérez-Boada *et al*., 2005). For VAO activity, the reaction mixture contained 125 μL of 1mM veratryl alcohol, 375 μL of 0.25 M sodium tartrate buffer, pH 5 and 400 μL of water and 100 μL of EE. VAO activity was followed by absorbance increase at 310 nm (ε=9300 cm^{-1} M^{-1}) (Bourbonnais and Paice, 1989). DyP activity was measured in the assay mixture that contained 850 μL of substrate (2.5 mM ABTS) in 0.1 M sodium tartrate buffer, pH 5.0, 100 μL of EE and 50 μL of H_2O_2, the activity was determined after incubating at 45ºC for 1 min and observing the absorbance at 418 nm (ε=36000 cm^{-1} M^{-1}) (Salvachúa *et al*., 2013).

3 Results and discussion

The cavity amino acids found by CASTp were calculated to a test radius of 1.4 Å, as CASTp finds all the cavities of the proteins, these cavities were cleaned first, removing the amino acids that were in direct coordination with the copper atoms in the case of laccase and with the heme group for DyP, MgP and VP, and afterwards using the UniProt database to confirm that in said cavities there were amino acids delimited as "active site or metal binding" but that in turn These will not make up part of the "structuring" amino acids that bind the copper or iron atoms (Table 1). Figure 1 shows the growth of *Pleurotus ostreatus* obtaining X_{max} values of 5.90 and 6.89 g L^{-1} for SSF and SmF, respectively. SSF had higher μ value (0.055 h^{-1}) than SmF (0.022 h^{-1}). The growth of any organism is influenced by the conditions of the fermentative system due to intrinsic development conditions (Pereira *et al*., 2007; Téllez-Téllez *et al*., 2008; Díaz *et al*., 2013), as well as, the composition and pH of the culture medium, temperature, presence of xenobiotics, oxygen availability, among others (Díaz *et al*., 2013; Velázquez *et al*., 2014; Díaz *et al*., 2014; Córdoba-Sosa *et al*., 2014; Camacho-Valenzuela *et al*., 2015).

Tabla 1. Flexible cavity amino acids for molecular docking calculations.

Lac	MnP	VP	DyP
VAL182	GLU37	GLU37	GLY213
PRO183	HIS40	HIS40	GLN214
HIS184	GLU41	GLU41	ASP215
ASP225	GLY87	ALA174	PRO216
SER226	ASP90	ASP176	ILE217
ASN227	ALA180	GLY184	ARG218
ASN283	GLN181		ASN313
SER 284	ASP182		LYS314
GLY412	GLY190		PHE315
PRO413			ASP316
HIS414			TYR339
ASP449			ARG341
ILE473			ASN342
HIS476			GLU345
			ASP354
			ARG357

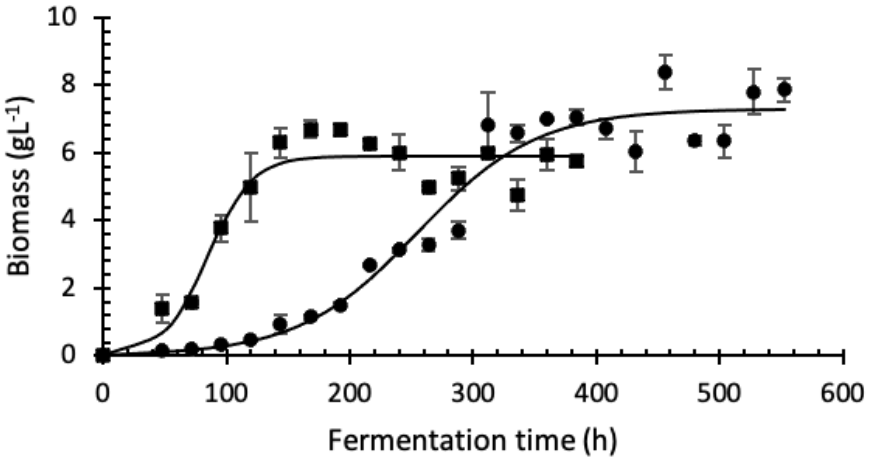

Fig. 1. Growth of *Pleurotus ostreatus* in SSF (■) and SmF (●). The bars represent the standard deviation of three replicates.

Several studies show differences in the μ and X_{max} values in strains of the same genus of fungi; apparently, the strain used and the growth conditions determine these values. Díaz *et al*. (2011a) studied five different strains of *Pleurotus ostreatus* developed in SmF, observing X_{max} values of 8.2, 7.2, 7.1, 6.1 and 2.3 g L^{-1} of the Po83, Po7, Po37, Po52 and Po3 strains respectively. Díaz *et al*. (2011b) observed an X_{max} of 4.62 g L^{-1} for the strain 32783 of *Pleurotus ostreatus*, and Velázquez *et al*. (2014), observed that this same strain but cultivated in SSF has an X_{max} of 3.7 g L^{-1}. Téllez-Téllez *et al*. (2008), reported for the strain 32783 of *Pleurotus ostreatus* an X_{max} of 4.5 and 5.5 gL^{-1} in SSF and SmF respectively. Likewise, Córdoba-Sosa *et al*. (2014), observed that *Pleurotus ostreatus* strain ARS 3625 had an X_{max} of 8.78 g L^{-1} when grown in SmF in the presence of di (2-ethylexyl) phthalate. Unlike this study, this last strain showed an intermediate range in the values of X_{max} (5.9 and 6.89 g L^{-1} in SSF and SmF respectively), these data suggest that the development conditions, the strain and the use of xenobiotics modifies biomass production.

Regarding the values of μ, different values have been reported both in SmF and SSF, even being in strains of the same genus of fungi, for example, values of 0.026, 0.020, 0.018, 0.012, 0.007, 0.016, 0.033 and 0.034 h^{-1} were observed for *Pleurotus ostreatus* strains (Díaz *et al*., 2011a; Díaz *et al*., 2011b; Velázquez *et al*., 2014; Córdoba-Sosa *et al*., 2014; Téllez-Téllez *et al*., 2008), unlike this study in which a μ of 0.055 h^{-1} was observed for SSF, which it was higher compared to other previous studies and for SmF it was 0.022 h^{-1}, similar to that previously reported; this suggests that the strain, the development conditions and the composition of the culture medium are the main reasons to explain these differences.

SmF and SSF are the most studied and controlled metabolite production systems, however, there are few reports on the kinetic parameters of growth and production of oxidase enzymes of the *Pleurotus ostreatus* ARS 3526 strain, and there are no reports on the molecular docking of oxidases produced by this species of fungus.

Figure 2 shows the activity and molecular docking of Lac. The maximum values of Lac activity were 24.67 UL^{-1} (17593.3 AU L^{-1}) and 11.74 UL^{-1} (8373.3 AU L^{-1}) for SSF at 144 h and for SmF at 312 h of growth, in both cases at the end of the exponential phase. *Pleurotus ostreatus* is a fungus used in the study of Lac production in both SSF and SmF, it has also been reported that the enzymatic activity depends on the strain of fungus used, composition of the culture medium, use of inducers, aeration, pH of the culture medium, temperature, among other factors (Téllez-Téllez *et al*., 2008; Díaz *et al*., 2014). In this research, the activity value of Lac in SSF was approximately twice that in SmF, it is important to say that in both bioprocesses, the highest activity values were observed at the end of the exponential phase. Karp *et al*. (2015) reported Lac activity up to 11.45 UL^{-1} produced by *Pleurotus ostreatus* Pl 22 Em grown in SSF, which was just under half of that obtained in the same fermentation system of this investigation.

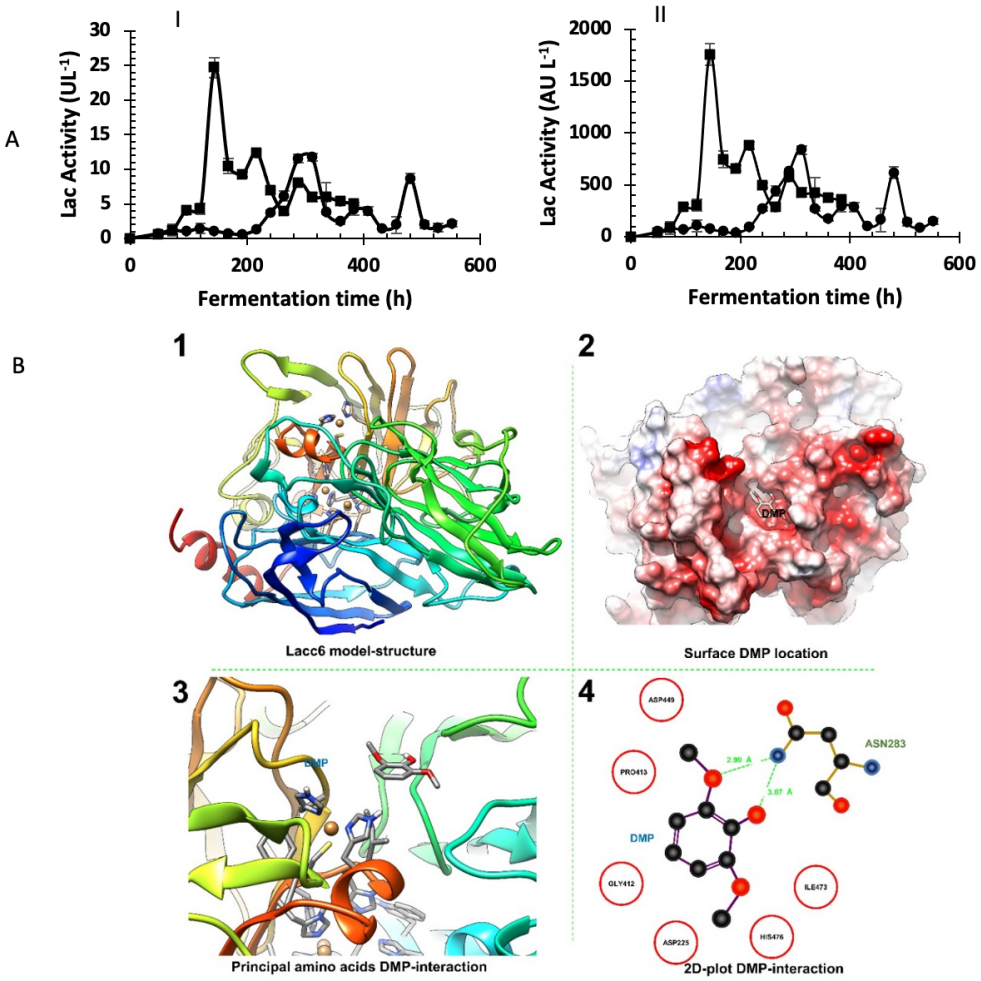

Fig. 2. Lac activity (A) and molecular docking of laccase (B). Lac activity *Pleurotus ostreatus* grown in SSF (■) and SmF (•) reported in UL^{-1} (I) and AU (II), bars represent the standard deviation of three replicates. For molecular docking, in the schematic cartoon representation of molecular modelling of Lacc 6 structure, the tetra-nuclear active site is represented in stick, in spheres are the copper ions, from red to blue color are signpost the N-ter and C-ter (1). Surface section of Lacc 6 protein, in red color showed the surface area cavity that host the interaction between the Lacc 6 and DMP ligand (2). Three-dimensional representation of Lacc 6 between interaction key residues with DMP ligand, DMP and R amino acid group are shows in stick, and in cartoon secondary structure of Lacc 6 (3). Ligplot of DMP-Lacc 6 interaction, green and magenta lines represent the Hydrogen bond, hydrophobic interactions, and its length, respectively, and the proximal residues to DMP are in red circle (4).

For this same activity from *Pleurotus ostreatus*, but informed in AU, the SSF was approximately 0.44 times higher than those reported by Velázquez *et al*. (2014) and seven times higher than that reported by Téllez-Téllez *et al*. (2008) In SmF of this research, the Lac activity (AU) was 2.6 times greater regarding the reported by Díaz *et al*. (2011a), but 4.5 and 8.4 times smaller than that observed by Díaz *et al*. (2011b) and Díaz *et al*. (2013), respectively. The differences in the Lac activity values could be, among other factors, the strain used and the pH of the culture medium. In the molecular docking predicted complex, was assumed to be a system closer to the native state of the complex. For four complexes each ligand was docked to the sites predicted with Caver, CASTp, Active site in UniProt and compared to crystallographic structures depicted in the PDB. The root means square deviation RMSD scores of ligand conformation predicted by ABTS,

DMP and Mn-ion was minus of 1.0 Å. As shown, the Lacc 6-DMP complex represented in Figure 2B4 is stabilized by two hydrogen bonds between ASN283 and ligand DMP, and the pocket cavity consists ASP225, GLY412, PRO413, ASP449, ILE473 and HIS476, the last HIS476 connects directly to the tetranuclear cluster of the active site and in this place the DMP molecule can be oxidized. Figure 2B (4) shows a two-dimensional map for the docking of the DMP substrate with Lacc6 in the active site cavity, shows that the hydroxyl group of C1 and carbonyl of C6 are linked to the amine group (NH2) of ASN283, which is one of the amino acids adjacent to the active site, by means of two bifurcated hydrogen bonds (green color) at a distance of 2.99 Å in the oxygen of the carbonyl group and 3.07 Å of the oxygen of the carboxyl group, this hydrophobic residue plays a major role in the oxidation of DMP. Due to the composition of the surface, DMP has an easy access to HIS476 which suggests that it may be a primary electron acceptor, which would play a role for HIS476 in electron transfer. In the same way, DMP is involved in a semi-hydrophobic environment as it is located in the vicinity of amino acids ILE473 and PRO413. DMP is shown to be linked to amino acids coaxial to the active site of Lacc6 on the surface and not directly to copper T1.

The MnP activity, for both fermentations, the highest values were obtained around 100 h of fermentation (Figure 3A); It was observed that for SSF, this time corresponds to the exponential phase and for the case of SmF the maximum activity was in the adaptation phase of the fungus. The highest MnP activity obtained in the SSF was 10.12 U L^{-1} and in the SmF the value was little more than 4 times higher (44.9 U L^{-1}).

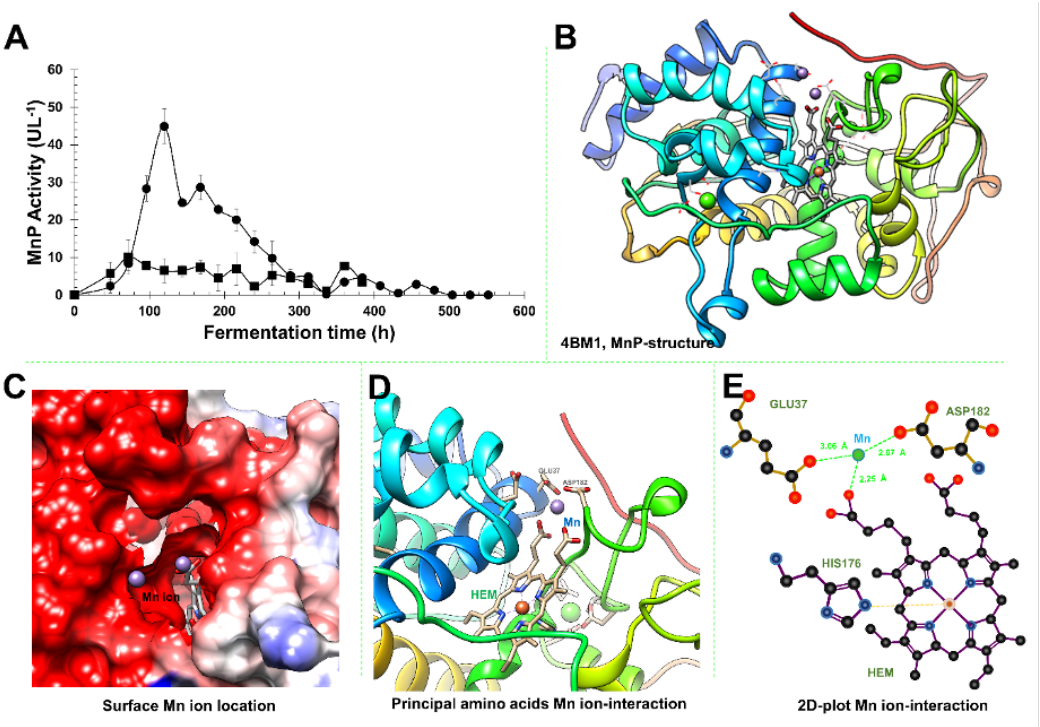

Fig. 3. MnP activity (A) and molecular docking (B-E). MnP of *Pleurotus ostreatus* grown in SSF (■) and SmF (●), bars represent the standard deviation of three replicates. B) Schematic cartoon representation of 4BM1 crystallographic structure, the Hemo group is represented in stick and the N-ter and C-ter are indicated from red to blue color. C) Surface section of MnP protein, in color red is showed the surface area cavity that host the interaction between the MnP and the MnP-ion. D) Three-dimensional representation of the interaction between MnP key residues and Mn-ion, in sphere are the Mn-ion, the Heme and R group are in stick. E) Ligplot of Mn-MnP, in green and magenta lines is represent the Hydrogen bond, hydrophobic interactions and its length, respectively.

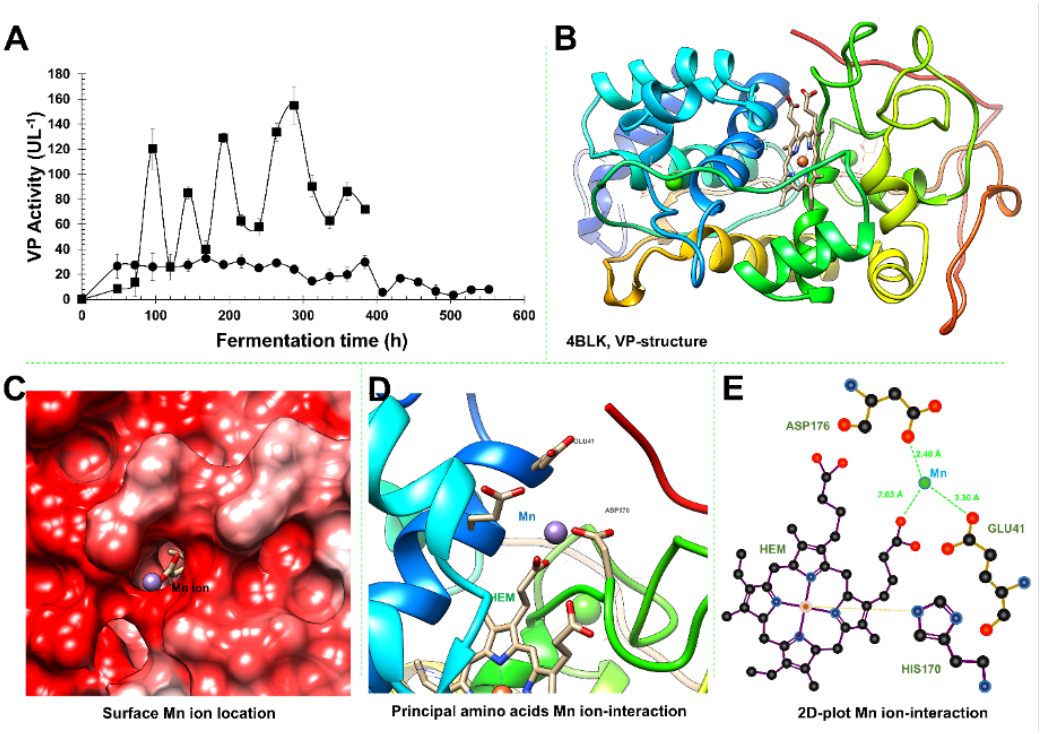

Fig. 4. VP activity (A) and molecular docking (B-E). VP activity of *Pleurotus ostreatus* grown in SSF (■) and SmF (●), bars represent the standard deviation of three replicates. B) Cartoon representation of 4BLK VP crystallographic structure, in the center of protein is the Hemo group, and from blue to red colors is indicated the N-ter to C-ter. C) VP surface protein, in red color is showed the surface cavity, the purple Mn-ion is inside the cavity pocket. D) 3D image of key residues between to Mn-ion. E) 2D interaction plot build with Ligplot by Mn-ion and VP, in green and magenta lines is represent the Hydrogen bond, hydrophobic interactions and its length, respectively.

Figure 4A shows the VP activity, with a different behavior between both fermentations. In the SSF a maximum value of 155 UL^{-1} was observed at 288 h which corresponds to the stationary phase, while in the SmF, the maximum value was 32.7 U L^{-1} at 168 h of fermentation which corresponds to the beginning of the exponential phase. Figures 3B-E and 4B-E show the Mn-ion complex with MnP and VP, respectively; the Mn-ion is stabilized through a bidentate coordination forming metal-oxygen bonds of glutamic and aspartic residues, the GLU37 or GLU41 and ASP182 and ASP176 to MnP and VP complex respectively, in addition, this same ion presents a monodentate metal-oxygen interaction with the oxygen (O) bonding of the carboxyl groups of the Heme group. In Figures 3E and 4E, a two-dimensional map for the docking of the Mg^{2+} ion with MnP and VP in the active site cavity is shown; the green color shows the Mn-ion where the coordination sphere of the ion reaches the carboxyl group of the amino acids GLU37, ASP182 and the Heme group for MnP and GLU41, ASP176 and the Heme group for VP. Likewise, a bidentate coordination is observed between the amino acids GLU37 and ASP192 (3.06 and 2.67 Å respectively for MnP) and GLU41 and ASP176 (3.30 and 2.46 Å respectively for VP), both Mn-O contacts probably on the first coordination sphere, this same diagram shows a monodentate Mn-O interaction with an O of the carboxyl in the Heme group (2.25 A and 2.03 A for MnP and VP respectively). HIS176 (for MnP) and HIS170 (for VP) are interacting with the Heme group, which may be involved in the transfer of electrons in the oxidoreductive action of both enzymes.

In this investigation, the MnP activity obtained in SmF was 16 times lower (730 U L^{-1}) than that reported by Retes-Pruneda (2014) for *Pleurotus ostreatus* 7992. On the other hand, Elisashvili *et al*. (2008) reported an MnP activity produced by *Pleurotus ostreatus* 2191 in SSF, 20% lower than that observed in this research. *Pleurotus ostreatus* and other basidiomycete fungi are capable of constitutively

producing VP, however, the production and activity can be increased by the presence of xenobiotics (Bibbins-Martínez *et al*., 2014; González-Caloch *et al*., 2015; Camacho-Valenzuela *et al*., 2015; Cruz-Pacheco *et al*., 2015). In this work, the VP activity for SSF was 4.7 times higher with respect to SmF, but 10 times lower than that reported by Cruz-Pacheco *et al*., (2015) for *Pleurotus ostreatus* 32783 developed in the presence of textile dyes.

The activity and molecular docking of DyP from *Pleurotus ostreatus* is shown in Figure 5. In SSF, an increase in activity was observed over time, and it remained almost constant during the stationary phase of growth of the fungus; the maximum activity value was 5.26 UL^{-1} at 168 h. In the case of SmF, the maximum activity value was 3.47 UL^{-1} at 480 h. On the other hand, the DyP-ABTS molecular docking presents two interactions, an ionic interaction between GLU345 and one nitrogen of the ABTS molecule, and the other, a hydrophobic interaction between ASP354 and ABTS sulfonic acid. DyPs are classified in the family of the peroxidase-cyclooxygenase type 1, which includes bacterial peroxidases; these enzymes oxidize many dyes, particularly anthraquinone-derived xenobiotics, phenolic compounds such as ABTS (Sugano, 2009; Sugano *et al*., 2009). Figure 5E shows the two-dimensional map for the docking of the ABTS ligand with DyP in the active site cavity, it is observed that the vicinity of the ABTS accommodation is hydrophobic and charged mediated by the residues TYR339, ARG 341, ASP316, PHE315, LYS314, ASP215 and GLY213. Two interactions are established by hydrogen bridge between ABTS and the cavity of the DyP, one of them through the oxygen of the carboxyl group of GLU345 with the central nitrogen of the ABTS molecule and the other between the phosphate group of ABTS and the group carboxyl of ASP354, each of them with a distance of 2.44 and 3.54 Åsrespectively, it is appreciated that the amino acids coaxial (red circles) to the molecular of ABTS play a fundamental role in the generation of an electrostatic environment favorable for the oxidoreduction of the ligand.

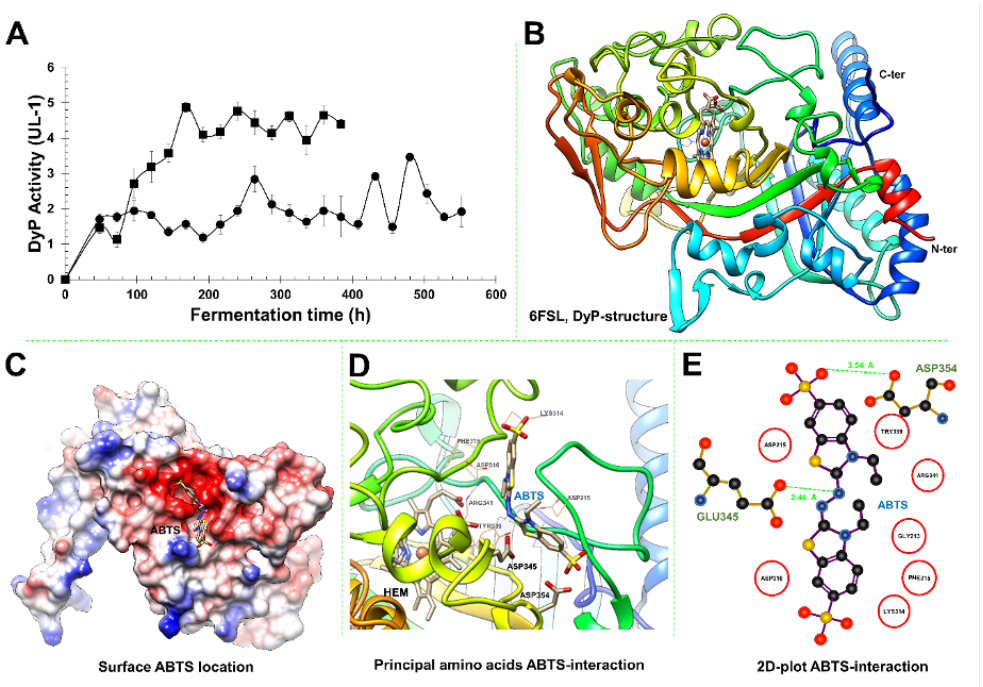

Fig. 5. DyP activity (A) and molecular docking (B-E). DyP activity of *Pleurotus ostreatus* grown in SSF (■) and SmF (●), bars represent the standard deviation of three replicates. B) Schematic cartoon representation of 6FSL crystallographic structure depicted in the Protein Data Bank, the Hemo group is represented by stick in the protein center, from blue to red color is marked the N-ter and C-ter. C) Surface of DYP protein, in red is depicted the pocket cavity to host the ABTS ligand. D) Three-dimensional interaction between DyP key residues and ABTS, is represented in, schematized in cartoons. E) Ligplot of ABTS-DyP interaction, green and magenta lines represent the ionic interaction, hydrophobic interactions and their length, respectively; in red circle are the proximal residues.

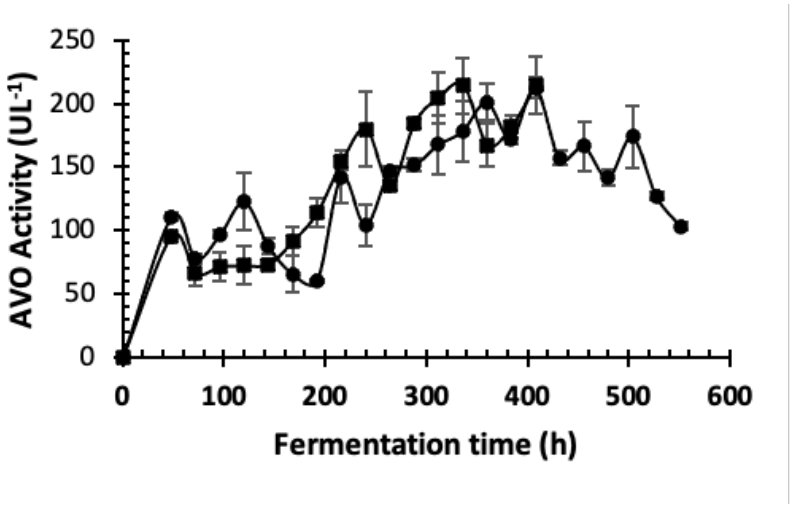

Fig. 6. VAO activity of *Pleurotus ostreatus* grown in SSF (■) and SmF (●).

Tabla 2. Descriptor of binding affinity by PRODIGY.

Complex	ΔGnoelec (Kcal/mol)
Lacasa-DMP	−6.7
MgP-Mg	− − −
VP-Mg	− − −
DyP-ABTS	−7.0

The ability to oxide synthetic colorants type anthraquinone, with high redox potential, that barely can be oxidized by other peroxidases, is a fundamental characteristic for all DyP studied until now (Kim and Shoda, 1999). However, very few studies have been focused to the production of this kind of enzymes by fungus organisms (Camacho-Valenzuela *et al*., 2015; Cuamátzi-Flores *et al*., 2015; González-Caloch *et al*., 2015; Díaz *et al*., 2014). The activity values obtained in this research for DyP were smaller than the obtained by other authors.

On the other hand, an approximation to the free energy was made, calculated with the PRODIGY server (PROtein binDIng enerGY prediction), having results for the DMP and ABTS ligands, for Mn it is not calculable.

Figure 6 shows the VAO activity of *Pleurotus ostreatus*, a similar pattern was observed in both bioprocesses, the maximum activity values (21.47 UL^{-1} for SSF and 21.25 UL^{-1} for SmF) were obtained in the final stage of growth. It is important to mention that there is no crystallographic structure of VAO enzymes from *Pleurotus ostreatus*, so the molecular docking could not be done. Very few studies have been carried out on VAO of *Pleurotus ostreatus* (Bourbonnais and Paice, 1988; Bourbonnais and Paice, 1989; Guillen *et al*., 1990; Sannia *et al*., 1991). These enzymes were first described in *Polystictus versicolor* by Farmen *et al*., (1960), are related to the lignin degradation processes, which many fungi can do constitutively. In this investigation, the maximum values of VAO activity in both systems were very similar and 0.37 times higher than those observed in *Pleurotus eryngii* by Guillén *et al*., (1990), and more than 20 times higher than that reported for the same activity of *Pleurotus sajor-caju* by Bourbonnais and Paice, (1988).

Conclusions

This is the first report about the molecular docking between Mn-ion, ABTS or DMP ligand with the respective oxidases of *Pleurotus ostreatus*. For the SSF the specific growth rate is 2.5 times higher regarding SmF, and, this fermentation system promotes the activity of Lac, VP and DyP. VAO activity was similar in both fermentation systems; MnP activity was higher in SmF and the maximum value was observed in different growth stage compared to SSF. This study offers the structural and functional details of the oxidases of *Pleurotus ostreatus*, in addition, the findings of the molecular docking showed that the examined ligands interacted with the enzymes mainly in negatively charged amino acids, which play a vital role in the oxidation-reduction process. The results of the computational coupling of Lac, MnP, VP and DyP with ABTS, DMP and Mn-ion.

Acknowledgements

Thanks to the Mexican Council of Science and Technology (CONACyT) for the scholarship for Maribel González Palma (No. 290789).

Nomenclature

Lac	Laccase
MnP	Manganese Peroxidase
VP	Versatile Peroxidase
VAO	Veratryl Alcohol Oxidase
DyP	Dye-Decolorizing Peroxidase
ABTS	2,2'-azino-bis(3-ethylbenzothiazoline-6-sulphonic acid)
ARS	Agricultural Research Service
DMP	2,6-dimethoxyphenol
NMP	Crystallography or nuclear magnetic resonance
PUF	Polyurethane foam
EE	Enzymatic extract
SmF	Submerged fermentation
SSF	Solid-state fermentation
U	International unit of enzymatic activity
PDA	Potato dextrose agar

References

Álvarez-Cervantes, J., Sánchez, C., Díaz, R., and Díaz-Godínez, G. (2016). Characterization of production of laccases, cellulases and xylanases of *Pleurotus ostreatus* grown on solid-state fermentation using an inert support. *Revista Mexicana de Ingeniería Química 15*, 323-331.

Bibbins-Martínez, M. D., Pérez-Parada, C., Nava-Galicia, S. B., Arroyo-Becerra, A., Villalobos-López, M. A., Díaz, R., and Díaz-Godínez, G. (2014). Enzymatic and expression profiling of oxidases produced by *Pleurotus ostreatus* in submerged fermentation in the presence of remazol brilliant blue R (RBBR) and yellow azo (AYG) dyes. *Journal of Chemical, Biological and Physical Sciences 4*, 17-25.

Bourbonnais, R., and Paice, M. G. (1988). Veratryl alcohol oxidases from the lignin-degrading basidiomycete *Pleurotus sajor-caju*. *Biochemical Journal 255*, 445-450.

Bourbonnais, R., and Paice, M. G. (1989). Oxidative enzymes from the lignin-degrading fungus *Pleurotus sajor-caju*. in: *Plant Cell Wall Polymers: Biogenesis and Biodegradation*, NG Lewis, MG Paice (ed.), ACS Symp Ser.

Camacho-Valenzuela, J., Nava-Galicia, S. B., Díaz, R., Tlecuitl-Beristain, S., Garrido-Bazán, V., and Bibbins-Martínez, M. D. (2015). Induction effect of azo yellow dye on gene expression and activity of oxidases of *Pleurotus ostreatus* grown in submerged fermentation. *Revista Latinoamericana el Ambiente y las Ciencias 6*, 57-71.

Chen, D., Menche, G., Power, T.D., Sower, L., Peterson, J.W., and Schein, C.H. (2007). Accounting for ligand-bound metal ions in docking small molecules on adenylyl cyclase toxins. *Proteins 67*, 593-605.

Córdoba-Sosa, G., Torres, J. L., Ahuactzin-Pérez, M., Díaz-Godínez, G., Díaz, R., and Sánchez, C. (2014). Growth of *Pleurotus ostreatus* ATCC 3526 in different concentrations of di (2-ethylhexyl) phthalate in submerged fermentation. *Journal of Chemical, Biological and Physical Sciences 4*, 96-103.

Cruz-Pacheco, S. K., Nava-Galicia, S. B., Díaz, R., and Bibbins Martínez, M. D. (2015). Expression profile of versatile peroxidase (VP) enzyme during grown of *Pleurotus ostreatus* in the presence of dyes. *Revista Latinoamericana el Ambiente y las Ciencias 6*, 30-43.

Cuamátzi-Flores, J. L., Nava-Galicia, S. B., Díaz, R., Garrido-Bazán, V., Tlecuitl-Beristain, S., and Bibbins-Martínez, M. D. (2015). Activity determination of the DyP enzyme produced by *Pleurotus ostreatus* and evaluation of their oxidative capacity on several textile dyes. *Revista Latinoamericana el Ambiente y las Ciencias 6*, 44-56.

Dávila-Vázquez, G., Tinoco, R., Pickard, M. A. and Vázquez-Duhalt, R. (2005). Transformation of halogenated pesticides by versatile peroxidase from *Bjerkandera adusta*. *Enzyme and Microbial Technology 35*, 223-231.

Díaz-Godínez, G., Soriano-Santos, J., Augur, C. and Viniegra-González, G. (2001). Exopectinases produced by Aspergillus niger in solid state and submerged fermentation: a comparative study. *Journal of Industrial Microbiology & Biotechnology 26*, 271-275.

Díaz, R., Alonso, S., Sánchez, C., Tomasini, A., Bibbins-Martínez, M. D., and Díaz-Godínez, G. (2011a). Characterization of the growth and laccase activity of strains of *Pleurotus ostreatus* in submerged fermentation. *Bioresources 6*, 282-290.

Díaz, R., Sánchez, C., Bibbins-Martínez, M. D., and Díaz-Godínez, G. (2011b). Effect of medium pH on laccase zymogram patterns produced by *Pleurotus ostreatus* in submerged fermentation. *African Journal of Microbiology Research 5*, 2720-2723.

Díaz, R., Téllez-Téllez, M., Sánchez, C., Bibbins-Martínez, M. D., Díaz-Godínez, G., and Soriano-Santos, J. (2013). Influence of initial pH of the growing medium on the activity, production and genes expression profiles of laccase of *Pleurotus ostreatus* in submerged fermentations. *Electronic Journal of Biotechnology 4*, 1-13.

Díaz, R., Nava-Galicia, S. B., Díaz-Godínez, G., and Bibbins-Martínez, M. D. (2014). Influence of yellow azo dye on the expression profile of phenoloxidases of *Pleurotus ostreatus* grown in submerged fermentation. *Journal of Chemical, Biological and Physical Sciences 4*, 51-58.

Díaz, R., Díaz-Godínez, G., Anducho-Reyes, M. A., Mercado-Flores, Y., and Herrera-Zúñiga, L. D. (2018a). In silico design of laccase thermostable mutants from Lacc 6 of *Pleurotus ostreatus*. *Frontiers in Microbiology 9*, 2743.

Díaz, R., Mercado-Flores, Y., Díaz-Godínez, G., Herrera-Zúñiga, L. D. Álvarez-Cervantes, J., and Anducho-Reyes, M. A. (2018b). In silico generation of laccase mutants from Lacc 6 of *Pleurotus ostreatus* and bacterial enzymes. *BioResources 13*, 8113-8131.

Elisashvili, V., Penninckx, M., Kachlishvili, E., Tsiklauri, N., Metreveli, E., Kharziani, T., and Kvesitadze, G. (2008). Lenitus edodes and Pleurotus species lignocellulolytic enzymes activity in submerged and solid-state fermentation of lignocellulosic wastes of different composition. *Bioresource Technology 99*, 457-462.

Farmen, V. C., Henderson, M. E. K., and Russell, J. D. (1960). Aromatic-alcohol-oxidase activity in the growth medium of *Polystictus versicolor*. *Biochemical Journal 74*, 257-262.

Fernández-Fueyo, E., Ruiz-Dueñas, F. J., Martínez, M. J., Romero, A., Hammel, K. E., Medrano, F. J., and Martínez, A. T. (2014). Ligninolytic peroxidase genes in the oyster mushroom genome: heterologous expression, molecular structure, catalytic and stability properties, and lignin-degrading ability. *Biotechnology for Biofuels 7*, 2.

Giardina, P., Palmieri, G., Fontanella, B., Rivieccio, V., and Sannia, G. (2000). Manganese peroxidase isoenzymes produced by *Pleurotus ostreatus* grown on wood sawdust. *Archives of Biochemistry and Biophysics 376*, 171-179.

González-Caloch, I., Nava-Galicia, S. B., Díaz, R., Garrido-Bazán, V., Tlecuitl-Beristain, S., and Bibbins-Martínez, M. D. (2015). Determination of oxidases activity produced by *Oxyporus latemarginatus* grown in submerged fermentation in the presence and the absence of the yellow azo dye. *Revista Latinoamericana el Ambiente y las Ciencias 6*, 72-88.

Grandes-Blanco, A. I., Díaz-Godínez, G., Téllez-Téllez, M., Delgado-Macuil, R. J., Rojas-López, M., and Bibbins-Martínez, M. D. (2013). Ligninolityc activity patterns of *Pleurotus ostreatus* obtained by submerged fermentation in presence of 2,6-dimethoxyphenol and remazol brilliant blue R dye. *Preparative Biochemistry & Biotechnology 43*, 468-480.

Guillen, F., Martínez, A. T., and Martínez, M. J. (1990). Production of hydrogen peroxide by aryl-alcohol oxidase from the ligninolytic fungus *Pleurotus eryngii*. *Applied Microbiology and Biotechnology 32*, 465-469.

Heberle, G., and de Acevedo, W. (2011). Bio-Inspired algorithms applied to molecular docking simulations. *Current Medicinal Chemistry 18*, 1339-1352.

Hernández-Ruiz, G. M., Álvarez-Orozco N. A., and Rios-Osorio, L. A. (2017). Bioremediation of organophosphates by fungi and bacteria in agricultural soils. A systematic review. *Ciencia & Tecnología Agropecuaria 18*, 138-159.

Herrera-Mora, J. A., Rosas-Acosta, J. M., Mercado, M., Martinez, M. M., and Pedroza, A. M.

(2004). Effect of the ligninolytic enzymes of the fungi Trametes versicolor and *Phanerochaete chrysosporum* immobilized in foam on the color removal, chemical demand of oxygen and chlorophenols in waste waters of the Colombian paper industry. *Universitas Scientiarum. 10*, 27-36.

Jurcik, A., Bednar, D., Byska, J., Marques, S. M., Furmanova, K., Daniel, L., Kokkonen, P., Brezovsky, J., Strnad, O., Stourac, J., Pavelka, A., Manak, M., Damborsky, J., Kozlikova, B. (2018). CAVER Analyst 2.0: Analysis and visualization of channels and tunnels in protein structures and molecular dynamics trajectories. *Bioinformatics bty386*.

Karp, S. G., Faraco, V., Amore, A., Letti, L. A. J., Soccol, V. T., and Soccol, C. R. (2015). Statistical optimization of laccase production and delignification of sugarcane bagasse by *Pleurotus ostreatus* in solid-state fermentation. *BioMed Research International 1-8*.

Kim, S. J., and Shoda, M. (1999). Purification and characterization of a novel peroxidase from *Geotrichum candidum* Dec 1 involved in decolorization of dyes. *Applied and Environmental Microbiology 65*, 1029-1035.

Knapp, J., Newby, P., and Reece, P. (1995). Decolorization of dyes by wood-rotting basidiomycete fungi. Enzyme and Microbial Technology 17, 664-668. Martínez-Restrepo, Y. M. 2014. *Selection of filamentous fungi with potency for the degradation of lignocellulose isolated from agro-industrial waste of coffee and castor*. Bachelor's degree, Catholic University of Manizalez, Manizales, Caldas, Colombia.

Medina, J. D. C., Woiciechowski, A. L., Guimaraes, L. R. C., Karp, S. G., and Soccol, C. R. (2017). Peroxidases, production, isolation and purification of industrial products. *Current Developments in Biotechnology and Bioengineering*, 217-232.

Montalvo, G., Téllez-Téllez, M., Díaz, R., Sánchez, C., and Díaz-Godínez, G. (2019). Isoenzymes and activity of laccases produced by *Pleurotus ostreatus* grown at different temperatures. *Revista Mexicana de Ingeniería Química 19*, 345-354.

Montoya, S., Sánchez, O. J., and Levin, L. (2014). Evaluation of endoglucanase, exoglucanase, lacasa and lignin peroxidase activities in ten white rot fungi. Biotechnology in the Agricultural and Agroindustrial Sector 12, 115-124.

Morris G. M., Lim-Wilby, M. (2008). Molecular docking. In: *Molecular Modeling of Proteins. Methods Molecular Biology*™, Kukol A. (eds), Humana Press.

Morris, G. M., Huey, R., Lindstrom, W., Sanner, M. F., Belew, R. K., Goodsell, D. S. and Olson, A. J. (2009). Autodock4 and AutoDockTools4: automated docking with selective receptor flexibility. *Journal of Computational Chemistry 30*, 2785-2791.

Olvera-García, C., Díaz-Godínez, G., Sánchez, C., Álvarez-Cervantes, J., Martínez-Carrera, D. and Díaz, R. (2017). Laccases from *Pleurotus ostreatus*. *Mexican Journal of Biotechnology 2*, 122-134.

Pagadala, N. S., Syed, K. and Tuszynski, J. (2017). Software for molecular docking: a review. *Biophysical Reviews 9*, 91-102.

Pereira, G., Herrera, J., Machuca, A., and Sánchez, M. (2007). Effect of pH on the in vitro growth of ectomycorrhizal fungi collected from *Pinus radiata* plantations. *Bosque 28*, 215-219.

Perez-Boada, M., Ruiz-Dueñas, F. J., Pogni, R., Basosi, R., Choinowski, T., Martínez, M. J., Piontek, K., Martínez, A. T. (2005). Versatile peroxidase oxidation of high redox potential aromatic compounds: Site-directed mutagenesis, spectroscopic and crystallographic investigation of three long-range electron transfer pathaways. *Journal of molecular biology 354*, 385-402.

Retes- Pruneda, J. L. (2014). *Bioremediation of vinegars from the tequila and mezcalera industry through physicochemical and biological treatment*. Doctor's Thesis, University Autonomous of Aguascalientes, Aguascalientes, Mexico.

Rodríguez, E., Nuero, O., Guillén, F., Martínez, A. T., and Martínez, M. J. (2004). Degradation of phenolic and non-phenolic aromatic pollutants by four *Pleurotus* species: the role of laccase

d versatile peroxidase. *Soil Biology and Biochemistry 36*, 909-916.

Romero, A., Davo-Siguero, I., Martinez, A.T. (2019). Structure of two mutants: F194Y and F194W of the Dye-decolorizing peroxidase DYP from *Pleurotus ostreatus*. (https://www.rcsb.org/structure/6FSL), accessd 08 May 2020.

Rothschild, N. Levkowitz, A. Hadar, Y., and Dosoretz, C. G. (1999). Manganese deficiency can replace high oxigen levels needed for lignin peroxidase formation by *Phanerochaete chrysosporium. Applied and Environmental Microbiology 65*, 483-488.

Ruiz-Dueñas, F. J., Lundell, T., Floudas, D., Nagy, L. G., Barrasa, J. M., Hibbett, D. S., and Martínez, A. T. (2013). Lignin-degrading peroxidases in Polyporales: an evolutionary survey based on 10 sequenced genomes. *Mycologia 105*, 1428-1444.

Sannia, G., Limongi, P., Cocca, E., Buonocore, F., Nitti, G., and Giardina, P. (1991). Purification and characterization of a veratryl alcohol oxidase enzyme from the lignin degrading basidiomycete *Pleurotus ostreatus*. *Biochimica et Biophysica Acta (BBA) General Subjects 1073*, 114-119.

Salvachúa, D., Prieto, A., Martínez, A. T., and Martínez, M. J. (2013). Characterization of a novel dye-decolorizing peroxidase (DyP)-type enzyme from Irpex lacteus and its application in enzymatic hydrolysis of wheat straw. *Applied and Environmental Microbiology 79*, 4316-4324.

Sugano, Y. (2009). DyP-type peroxidases comprise a novel heme peroxidase family. *Cellular and Molecular Life Sciences 66*, 1387-1403.

Sugano, Y., Matsushima, Y., Tsuchiya, K., Aoki, H., Hirai, M., and Shoda, M. (2009). Degradation pathway of an anthraquinone dye catalyzed by a unique peroxidase DyP from *Thanatephorus cucumeris* Dec 1. *Biodegradation 20*, 433-440.

Téllez-Téllez, M., Fernández, J., Montiel, A., Sánchez, C., Díaz-Godínez, G. (2008). Growth and laccase production by *Pleurotus ostreatus* in submerged and solid-state fermentation. *Applied Microbiology and Biotechnology 81*, 675-679.

Tian, W., Chen, C., Lei, X., Zhao, J., Liang, J. (2018). CASTp 3.0: computed atlas of surface topography of proteins. *Nucleic Acids Research 46*, W363-W367.

Pettersen, E. F., Goddard, T. D., Huang, C. C., Couch, G. S., Greenblatt, D. M., Meng, E. C., and Ferrin, T. E. (2004). UCSF Chimera–a visualization system for exploratory research and analysis. *Journal of Computational Chemistry 25*, 1605-1612.

Ullah, M. A., Kadhim, H., Rastall, R. A., and Evans, C. S. (2000). Evaluation of solid substrates for enzymes production by *Coliorus versicolor*, for use in bioremediation of chorophenols in aqueos effluents. *Applied Microbiology and Biotechonology 54*, 832-837.

UniProt Consortium. (2019). UniProt: a worldwide hub of protein knowledge. *Nucleic Acids Research 47*, D506-D515.

Valenzuela-Cobos, J. D., Grijalva-Endara, A., Marcillo-Vallejo, R., and Garcés-Moncayo M. F. (2020). Production and characterization of reconstituted strains of *Pleurotus* spp. cultivated on different agricultural wastes. *Revista Mexicana de Ingeniería Química 19*, 1493-1504.

Velázquez, L., Téllez-Téllez, M., Díaz, R., Bibbins-Martínez, M. D., Loera, O., Sánchez, C., Tlecuitl-Beristain, S., and Díaz-Godínez, G. (2014). Laccase isoenzymes of *Pleurotus ostreatus* grown at different pH in solid-state fermentation using polyurethane foam as support. *Annual Research & Review in Biology 4*, 2566-2578.

Villegas, E., Téllez-Téllez, M., Rodríguez, A., Carreón-Palacios, A.E., Acosta-Urdapilleta, M.L., Kumar-Gupta, V., and Díaz-Godínez, G. (2016). Laccase activity of *Pycnoporus cinabarinus* grown in different culture systems. *Revista Mexicana de Ingeniería Química 15*, 703-710.

Wallace, A. C., Laskowski, R. A. and Thornton, J. M. (1995). LIGPLOT: A program to generate schematic diagrams of protein-ligand interactions. *Protein Engineering, Design and Selection 8*, 127-134.